Wideband Dual-Polarized Filtering Antenna for Base Station Applications

Xuekang Liu, Benito Sanz-Izquierdo, Steven Gao, *Fellow, IEEE*, Lehu Wen, and Xue-Xia Yang

***Abstract*—A compact wideband dual-polarized filtering antenna based on tightly coupled cross dipoles is presented in this letter. The enhancement of impedance bandwidth is realized by introducing four impedance equalizers to equalize the input resistances of the two inherent resonant modes of tightly coupled cross dipole antenna. The enhancement of the selectivity is realized by introducing two radiation nulls in 5G sub-6 GHz n77 and n79 bands. The radiation null in n77 band is obtained by introducing the cross strips in the center of the antenna. The radiation null in the n79 band is achieved by the introduction of open-end branches. The manipulation of their key parameters allows for independent control over both radiation nulls. The validity of the antenna's design principle was confirmed by carrying out fabrication and measurements. The results obtained showcase the antenna's broad fractional bandwidth of 63.4% and exceptional port isolation of 31 dB. High out-of-band rejection levels in n77 and n79 bands are also obtained. In addition, since the whole radiator of the presented antenna is coplanar, it offers the advantage of a simple structure and convenient manufacturing, making it highly suitable for the use in base stations operating across multiple bands.**

***Index Terms*— Base station application, filtering antenna, wideband antenna, dual-polarized antenna.**

I. Introduction

DUAL-POLARIZED antennas have an extensive use in various wireless communication equipment [1], especially in base stations where frequency reuse and polarization diversity are essential. Some dual-polarized antennas were presented in [2]-[10] to cover the common frequency bands for 2/3/4G mobile communication systems (1710 MHz GHz- 2690 MHz). However, the frequency band (1427–1518 MHz) of international mobile telecommunication (IMT) services are not included in these designs. Serval dual-polarized antennas were proposed in [11]-[14] to cover all these desire frequency bands. However, none of them has the ability of suppressing out-of-band radiation.

Some filtering antennas were presented in [15]-[25] to reject the unwanted radiation. By combining the high-pass property of the ME dipole and the low-pass feeding network, a wideband dual-polarized antenna with bandpass response was presented in [18]. By employing modified dipole arms and differentially feed structure, a wideband dual-polarized filtering antenna with simple structure was proposed in [23]. This antenna has good gain suppression levels in 3.3-3.8 GHz and 4.8- 5.0 GHz. Although these antennas exhibit favorable impedance bandwidths and out-of-band rejection properties, none of them can encompass the desired 1.42-2.69 GHz frequency range while simultaneously achieving satisfactory gain suppression in the n77 (3.3-4.2 GHz) and n79 (4.8-5.0 GHz) bands.

This letter presents a novel design for a wideband dual-polarized filtering tightly coupled cross dipole antenna (TCCDA). The design incorporates impedance equalizers, cross strips, and open-end branches. The proposed antenna not only realizes a favorable operating bandwidth covering the targeted frequency range (1.42 - 2.69 GHz) but also provides effective gain suppressions in the 5G sub-6 GHz n77 and n79 bands. More importantly, the antenna allows for the independent adjustment of the two radiation nulls without influencing each other. All the radiator components are located on the same substrate layer, resulting in a simple and cost-effective fabrication process. These advantages make the proposed design an exceptional option for integrated base station applications.

II. Antenna Geometry and Design Concept

A. Antenna Geometry

The detailed geometry of the improved TCCDA is depicted in Fig.1. The whole radiator of this antenna are designed in the same plane, which makes it easy to fabricate. The impedance equalizers are utilized to improve the impedance bandwidth of the TCCDA to cover the target frequency range (1.42- 2.69 GHz). The cross strips and open-end branches strategically introduce two radiation nulls aimed at attenuating unwanted signals within the n77 band (3.3- 4.2 GHz) and the n79 band (4.8- 5.0 GHz). The cross dipoles are fed by the baluns. All the structures of the antenna are realized through PCB technology. Rogers 4003 substrates are utilized, featuring a dielectric constant of 3.55 and a loss tangent of 0.0027, with a thickness measuring 0.508 mm. All simulation results are derived through ANSYS HFSS, a commercial simulation software.

This work was supported in part by the Royal Society - International Exchanges 2019 Cost Share (NSFC) under Grant IEC\NSFC\191780, in part by Huawei Technologies Ltd, in part by Engineering and Physical Sciences Research Council (EPSRC) under Grant EP/S005625/1 and EP/N032497/1. (Corresponding author: Xuekang Liu.)

Xuekang Liu and Benito Sanz-Izquierdo are with the School of Engineering, University of Kent, Canterbury CT2 7NT, U.K. (e-mail: xl255@kent.ac.uk).

Steven Gao is with the Dept of Electronic Engineering, Chinese University of Hong Kong.

L. Wen is with the Department of Electronic and Electrical Engineering, Brunel University London, UB8 3PH, Uxbridge, U.K.

Xue-Xia Yang is with the School of Communication and Information Engineering, Shanghai University, Shanghai 200444, China.

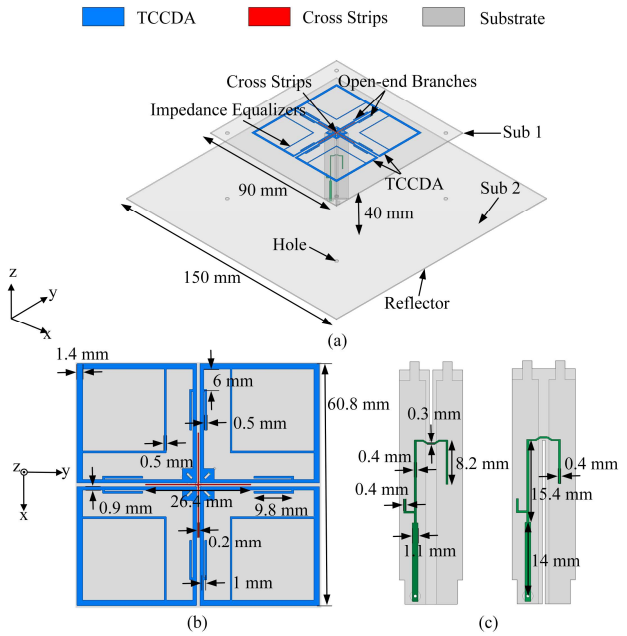

Fig. 1. The layout of the proposed design. (a) three-dimensional view, (b) overhead view, and (c) Balun configurations.

B. *Enhancement of Impedance Bandwidth*

Fig. 2 gives the simulated input impedance of the reference Ant.1 (traditional TCCDA, with reflector, without Baluns), Ant.2 (corner removed TCCDA), and Ant.3 (TCCDA with impedance equalizers). As can be seen in Fig. 2(a), there are two resistance peaks observed within the frequency range of 1 GHz to 3 GHz. However, the difference between the values of these two resistance peaks, with the peaks at 110 Ω and 1269 Ω respectively, is significant. It is obvious that these two resonant modes cannot be matched at the same time due to the large gap in the input resistance.

To explain why the Mode 2 has such a high input impedance, the simulated current distribution on Ant.1 at its resonant frequency is given in Fig. 3(a). According to the current distribution, the TCCDA can be categorized into two sections: the inner and outer parts. Since the current vectors on the adjacent inner parts of the dipole 1 and dipole 2 are with same amplitude and opposite direction. The inner parts can be seen as four sections of two-wire transmission lines (TL). They contribute little to the antenna's radiation due to the presence of reverse currents in proximity. The outer parts are the four corners of the TCCDA. As depicted in Fig. 3(a), when dipole 1 is excited, four nulls appear at the junctions between the inner and outer parts of dipole 2 due to the resonance of the outer parts in dipole 2. Therefore, at this frequency, the TCCDA can be equivalent to four two-wire TLs with one open-end (approximate open circuit). This is the reason why TCCDA has such a high input resistance at this frequency. This can also be verified by the input impedance of Ant. 2 in Fig. 2(a). It can be clearly seen that the removal of two corners from dipole 2 has minimal impact on the input impedance of TCCDA.

Through the analyze above, it can be found that there is an

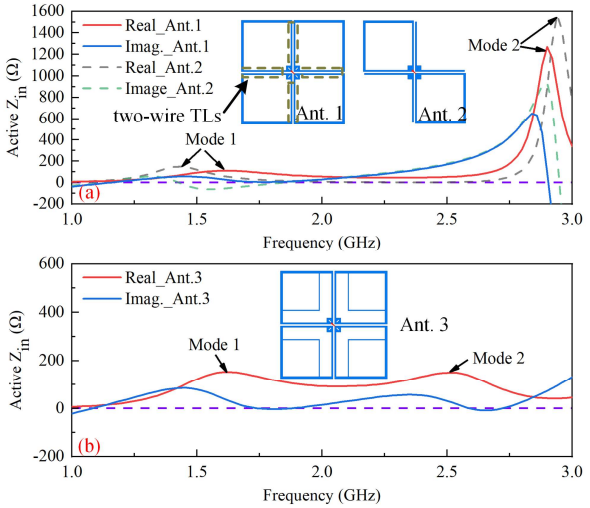

Fig. 2. Simulated input impedance of (a) reference antenna 1 and 2, and (b) reference antenna 3.

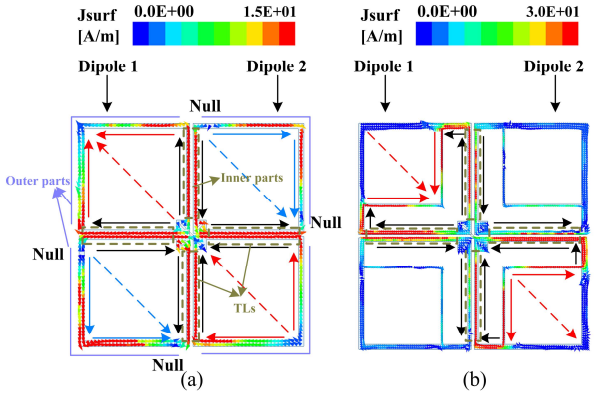

Fig. 3. Simulated current distribution on (a) reference Ant.1, and (b) reference Ant.3 at the resonant frequencies of Mode 2.

inherent limitation on the impedance of the TCCDA due to the existence of this high input impedance mode. Therefore, aiming to enhance the fractional bandwidth of the TCCDA, it is necessary to equalize the input resistances of these two modes. To address this issue, impedance equalizers are introduced. With the introduction of impedance equalizers, the energy is directed towards the impedance equalizer rather than the outer sections of the TCCDA, owing to the coupling between the inner parts and the impedance equalizers. Consequently, the outer parts in dipole 2 no longer resonate after the impedance equalizer is incorporated. As a result, the equivalent transmission lines no longer behave as open circuits, leading to a reduction in the input impedance of Mode 2. As depicted in Fig. 2(b), after introducing the impedance equalizers, the input resistance of the Mode 2 is reduced to the same level as the Mode 1, which allows us to easily match the antenna with a common Balun. As can be seen in Fig.3(b), when the dipole with -45° polarization (dipole 1) of Ant.1 is excited, the current distribution concentrates on the inner parts and the impedance equalizers.

C. *Enhancement of Selectivity*

To reduce or eliminate the mutual coupling between the

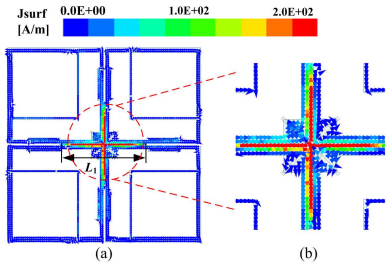

Fig. 4 (a) Simulated surface current distribution on the TCCDA and cross strips, and (b) the partially enlarged figure.

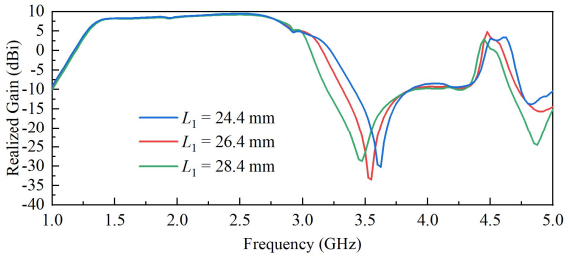

Fig. 5 The relationship between simulated realized gains and L_1.

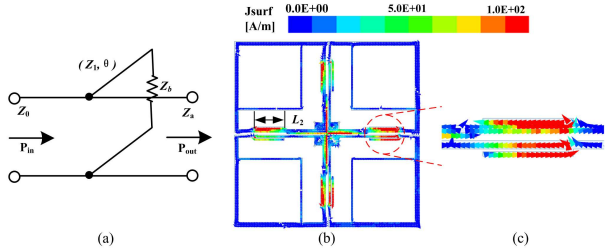

Fig. 6 (a) The transmission line representation of the open-end branch, (b) simulated surface current distribution on the TCCDA and cross strips, and (c) the partially enlarged figure.

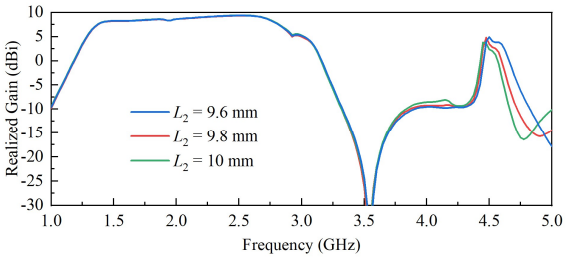

Fig. 7 The relationship between simulated realized gains and L_2.

antennas working in adjacent frequency bands, the antenna elements should also have good gain suppression characteristics. The radiation null in the n77 band is introduced by the cross strips. As illustrated in section II B, the inner parts of the TCCDA can be seen as transmission lines. The cross strips can be seen as resonators located next to them. Upon resonance of these resonators, a band-stop filter [26], [27] can be achieved. Thus, no power can be radiated into space within the working band of this band-stop filter.

Fig. 4(a) and (b) depict the simulated surface current distribution observed on the TCCDA and cross strips at 3.56 GHz (radiation null). At this frequency, the concentration of current density occurs mainly on the cross strips and the adjacent dipole arms. Besides, the directions of the current vectors in these two parts are opposite, causing the cancellation of the radiation. Thus, an attenuation in gain is expected at this at this frequency. The relationship between simulated realized gains and L_1 (length of the cross strips) is given in Fig.5. The Null 1 shift from 3.63 GHz to 3.46 GHz while the length of the cross strips change from 24.4 mm to 28.4 mm. The Null 2 keeps nearly unchanged despite variations in L_1.

The radiation null in the 5G sub-6 GHz n79 band is introduced by the open-end branches. Fig. 6 illustrates the transmission line representation of the open-end branches and the vector current distribution specifically on the radiator of our design at 4.86 GHz. As depicted in Fig. 6(a), the open-end branches can be equivalent to a section of open-end transmission line possessing an electrical length represented by θ and a characteristic impedance denoted by Z_1. The circuit's input impedance, Z_{in}, can be computed as:

$$Z_{in} = {}^{1}\Big/\left({}^{1}/_{Z_x} + {}^{1}/_{Z_a}\right) \tag{1}$$

Where Z_x can be calculated by:

$$Z_x = Z_1 \frac{Z_b + jZ_1 tan\theta}{Z_1 + jZ_b tan\theta} \tag{2}$$

When the electrical length $\theta = \pi/2$, Z_x can be expressed as:

$$Z_x = \frac{{Z_1}^2}{Z_b} \tag{3}$$

Since the branches in this design are open circuit ($Z_b = \infty$), we can get $Z_x = 0$. Thus, the input impedance $Z_{in} = 0$ when the electrical length of the open-end branches is $\frac{\pi}{2}$. The antenna can be seen as short circuited at this frequency. A radiation null can be realized.

In Fig. 6(b), and (c), the current density is mainly concentrated on the open-end branches at this frequency. Nearly no current can pass through them. A new radiation null is realized. Fig. 7 demonstrates that altering the length of the open-end branches can adjust the position of this radiation null without affecting Null 1.

The introduction of these two resonant zero points gives the antenna excellent radiation suppression characteristics in the 5G sub-6 GHz n77 and n79 bands. Moreover, both radiation nulls can be independently controlled by adjusting key parameters. This greatly reduces the complexity associated with the design of dual-polarized filtering antennas.

III. Results and Discussion

An experimental model of the novel TCCDA was made and tested to validate the design method. Using the Keysight P9377B Vector Network Analyzer, the S-parameters of the prototype were acquired. Subsequently, the antenna gain and normalized radiation patterns of the prototype were obtained in the antenna lab's anechoic chamber at the University of Kent.

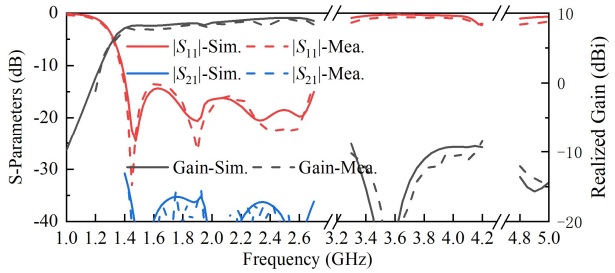

Fig. 8 $|S_{11}|$, $|S_{21}|$, and boresight realized gain of the proposed design obtained from simulation and measurement.

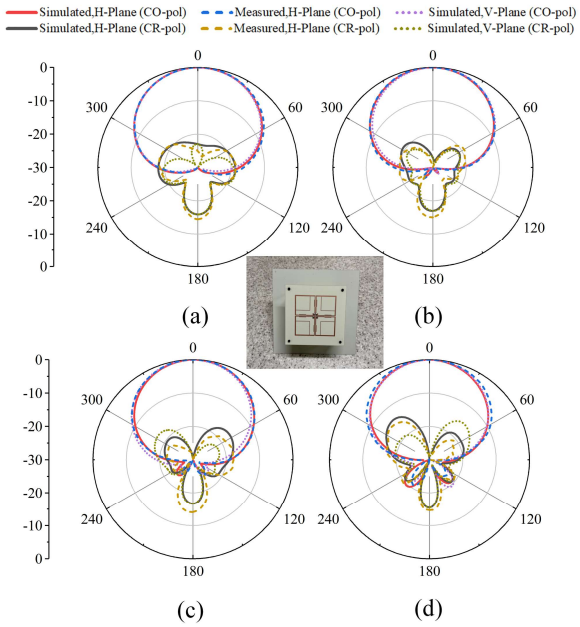

Fig. 9 Normalized radiation patterns obtained from simulation and measurement. (a) 1.4 GHz, (b) 1.8 GHz, (c) 2.2 GHz, and (d) 2.6 GHz.

Fig. 8 displays the S-parameters and realized gains obtained from both measurements and simulations. An extensive impedance bandwidth of 63.4%, spanning from 1.4 GHz to 2.7 GHz, is achieved, maintaining a reference of $|S_{11}| < -13.5$ dB. The measured $|S_{21}|$ is lower than -31 dB. Fabrication errors primarily contribute to the differences between the measured and simulated outcomes. Besides, the data in Fig. 8 reveal that the average gain of the prototype is 8.4 dBi within its operational frequency band.

The normalized radiation patterns (H-plane: yoz and V-plane: xoz) of the proposed design obtained from the simulation and measurement are shown in Fig. 9. Due to the symmetry of the antenna, only the measured radiation patterns within the horizontal plane (H-plane) are provided for brevity. These patterns demonstrate a notable agreement between the simulated and measured results. The proposed antenna exhibits a consistent and stable radiation pattern within its designated operating frequency band. Notably, across the operational frequency band, the Half-Power Beamwidth for this design falls between 67° and 81°. Additionally, the measured co-polarization remains 25 dB higher than its cross-polarization in the boresight direction.

TABLE I
COMPARISON OF THE WIDEBAND DUAL-POLARIZED ANTENNAS

Ref.	Size (λ_L^3)	BW (GHz;dB)	Layer	Gain (dBi)	Rej. (dB)
[7]	0.40×0.40×0.20	1.66-2.75 ($\|S_{dd11}\|$<-15) 49.4%	3	~8.7	/; /
[12]	0.31×0.31×0.24	1.39-2.80 ($\|S_{11}\|$<-15) 67%	6	~9	/; /
[21]	0.28×0.28×0.19	1.70-2.81 ($\|S_{11}\|$<-14) 49.2%	2	~7.6	12.6:3.3-4.2 21.6:4.8-5.0
[22]	0.33×0.33×0.16	1.55-2.45 ($\|S_{11}\|$<-10) 45.0%	1	~8.5	20.0:3.3-3.7 / :4.8-5.0
[23]	0.36×0.36×0.21	1.69-2.87 ($\|S_{dd11}\|$<-14) 51.8%	2	~8.5	13.1:3.3-3.8 18.9:4.8-5.0
[24]	0.30×0.30×0.18	1.65-2.75 ($\|S_{11}\|$<-15) 50.8%	1	~8.1	16.0 :3.3-4.2 22.1:4.8-5.0
[25]	0.28×0.28×0.19	1.70-3.01 ($\|S_{dd11}\|$<-15) 55.6%	2	~8.3	18.4 :3.3-4.2 / :4.8-5.0
Pro.	0.28×0.28×0.19	1.40-2.70 ($\|S_{11}\|$<-13.5) 63.4%	**1**	**~8.4**	16.8 :3.3-4.2 20.4 :4.8-5.0

* λ_L represents the wavelength at the lowest frequency in free space. Iso. means isolation. Rej. is rejection level in in n77 and n79 bands.

Table I presents a comparison between the proposed design and various previously presented wideband dual-polarized designs. As can be observed, the antennas in [7] has relatively larger size and narrower bandwidth than the proposed design. The antennas in [12] realize a broader impedance bandwidth compared to the proposed design. However, it doesn't have the ability of rejecting the unwanted signals. The designs in [21]-[25] obtain efficient attenuation of unwanted signals within targeted frequency range. However, none of them can cover the target frequency bands (1.42- 2.69 GHz). In summary, the presented design achieves a broader fractional bandwidth and superior selectivity in a more compact size and simpler structure.

IV. CONCLUSION

A novel wideband dual-polarized filtering TCCDA is proposed by introducing the impedance equalizers, the cross strips, and the open-end branches. By introducing the impedance equalizers, the input impedance of the TCCDA can be optimized to obtain a wider impedance bandwidth. Introducing cross strips in the center of the cross dipoles enables the attainment of a radiation null within the n77 band. For further improvement in rejecting out-of-band signals within the n79 band, four pairs of open-end branches are connected to the arms of the cross dipoles. With the ability to cover the desired frequency band of 1.42-2.69 GHz, the proposed antenna also showcases excellent gain suppression within the n77 and n79 bands. The combination of these benefits makes the proposed TCCDA a highly suitable option for integrated base station applications.

REFERENCES

[1] K.-L. Wong, "Compact and Broadband Microstrip Antennas," Hoboken, NJ, USA: Wiley, 2002, p. 10.

[2] Y. Gou, S. Yang, J. Li and Z. Nie, "A compact dual-polarized printed dipole antenna with high isolation for wideband base station applications," IEEE Trans. Antennas Propag., vol. 62, no. 8, pp. 4392-4395, Aug. 2014.

[3] Y. Luo, Q. -X. Chu and D. -L. Wen, "A plus/minus 45 degree dual-polarized base-station antenna with enhanced cross-polarization discrimination via addition of four parasitic elements placed in a square contour," IEEE Trans. Antennas Propag., vol. 64, no. 4, pp. 1514-1519, April 2016.

[4] S. -G. Zhou, Z. -H. Peng, G. -L. Huang and C. -Y. -D. Sim, "Design of a novel wideband and dual-polarized magnetoelectric dipole antenna," IEEE Trans. Antennas Propag., vol. 65, no. 5, pp. 2645-2649, May 2017.

[5] W. Chen et al., "A low profile broadband dual-polarized base station antenna using folded dipole radiation element," *IEEE Access*, vol. 7, pp. 67679-67685, 2019.

[6] L. -H. Wen et al., "A wideband differentially driven dual-polarized antenna by using integrated six-port power divider," IEEE Trans. Antennas Propag., vol. 67, no. 12, pp. 7252-7260, Dec. 2019.

[7] Z. Tang, J. Liu, Y. -M. Cai, J. Wang and Y. Yin, "A wideband differentially fed dual-polarized stacked patch antenna with tuned slot excitations," IEEE Trans. Antennas Propag., vol. 66, no. 4, pp. 2055-2060, April 2018.

[8] Z. Bao, Z. Nie and X. Zong, "A novel broadband dual-polarization antenna utilizing strong mutual coupling," IEEE Trans. Antennas Propag., vol. 62, no. 1, pp. 450-454, Jan. 2014.

[9] C. Ding, H. Sun, R. W. Ziolkowski and Y. J. Guo., "Simplified tightly-coupled cross-dipole arrangement for base station applications," *IEEE Access*, vol. 5, pp. 27491-27503, 2017.

[10] L. -H. Wen et al., "Compact dual-polarized shared-dipole antennas for base station applications," *IEEE Trans. Antennas Propag*., vol. 66, no. 12, pp. 6826-6834, Dec. 2018.

[11] L. Wu, R. Li, Y. Qin and Y. Cui, "Bandwidth-enhanced broadband dual-polarized antennas for 2G/3G/4G and IMT services," *IEEE Antennas Wireless Propag. Lett*., vol. 17, no. 9, pp. 1702-1706, Sept. 2018.

[12] Y. Cui, L. Wu and R. Li, "Bandwidth enhancement of a broadband dual-polarized antenna for 2G/3G/4G and IMT base stations," *IEEE Trans. Antennas Propag*., vol. 66, no. 12, pp. 7368-7373, Dec. 2018.

[13] L. H. Ye, X. Y. Zhang, Y. Gao and Q. Xue, "Wideband dual-polarized four-folded-dipole antenna array with stable radiation pattern for base-station applications," *IEEE Trans. Antennas Propag*., vol. 68, no. 6, pp. 4428-4436, June 2020.

[14] S. Martin-Anton and D. Segovia-Vargas., "Fully planar dual-polarized broadband antenna for 3G, 4G and Sub 6-GHz 5G base stations," *IEEE Access*, vol. 8, pp. 91940-91947, 2020.

[15] X. Liu et al., "A mutual-coupling-suppressed dual-band dual-polarized base station antenna using multiple folded-dipole antenna," *IEEE Trans. Antennas Propag.,* vol. 70, no. 12, pp. 11582-11594, Dec. 2022.

[16] W. Yang, M. Xun, W. Che, W. Feng, Y. Zhang and Q. Xue., "Novel compact high-gain differential-fed dual-polarized filtering patch antenna," *IEEE Trans. Antennas Propag*., vol. 67, no. 12, pp. 7261-7271, Dec. 2019.

[17] C. F. Ding, X. Y. Zhang, Y. Zhang, Y. M. Pan and Q. Xue., "Compact broadband dual-polarized filtering dipole antenna with high selectivity for base-station applications," *IEEE Trans. Antennas Propag*., vol. 66, no. 11, pp. 5747-5756, Nov. 2018.

[18] Y. Zhang, X. -Y. Zhang and Q. -H. Liu., "Dual-polarized filtering magnetoelectric dipole antenna utilizing intrinsic highpass filter network and integrated lowpass filter network," *IEEE Trans. Antennas Propag*., vol. 69, no. 12, pp. 8090-8099, Dec. 2021.

[19] L. -H. Wen et al., "A compact wideband dual-polarized antenna with enhanced upper out-of-band suppression," *IEEE Trans. Antennas Propag.*, vol. 67, no. 8, pp. 5194-5202, Aug. 2019.

[20] C. Zhang, Y. Zhang, X. Dai and Z. Yan., "A dual-polarized broadband high gain base station antenna with an octagonal structure," *IEEE Access*, vol. 11, pp. 35984-35992, 2023.

[21] L. -H. Wen et al., "A wideband differentially fed dual-polarized antenna with wideband harmonic suppression," *IEEE Trans. Antennas Propag*., vol. 67, no. 9, pp. 6176-6181, Sept. 2019.

[22] K. Huang, Y. Zhang and Q. H. Liu, "Dual-polarized filtering antenna based on a second-order SIR filter," *IEEE Antennas Wireless Propag. Lett*., doi: 10.1109/LAWP.2023.3320655.

[23] X. Liu, B. Sanz-Izquierdo, H. Zhang and S. Gao, "A wideband dual-polarized filtering antenna for multi-band base station application," in *Proc. 17th Eur. Conf. Antennas Propag.,* 2023, pp. 1-5.

[24] S. J. Yang, Y. F. Cao, Y. M. Pan, Y. Wu, H. Hu and X. Y. Zhang, "Balun-fed dual-polarized broadband filtering antenna without extra filtering structure," *IEEE Antennas Wireless Propag. Lett*., vol. 19, no. 4, pp. 656-660, April 2020.

[25] X. Liu et al., "A compact dual-polarized filtering antenna with steep cut-off for base-station applications," *IEEE Trans. Antennas Propag*., vol. 70, no. 7, pp. 5941-5946, July 2022.

[26] J.-S. G. Hong and M. J. Lancaster, *Microstrip Filters for RF/Microwave Applications.* New York, NY, USA: Wiley, 2001. P.169.

[27] Z. J. Xiao, Y. F. Cao, J. S. Lin, Y. Lan and Q. Xue, "Dual-band shared-aperture base-station antenna array with dual polarization using filtering magnetoelectric dipole antenna," *IEEE Open J. Antennas Propag.*, doi: 10.1109/OJAP.2023.3333905.